Supplementary Information

Dynamic response and roughening of ferroelectric domain walls driven at planar electrode edges

Guillaume Rapin,* Sophia Ehrensperger,† Cédric Blaser,‡ Nirvana Caballero, and Patrycja Paruch
Department of Quantum Matter Physics, University of Geneva, 1211, Geneva, Switzerland
(*patrycja.paruch@unige.ch)
(*nirvana.caballero@unige.ch)
(*guillaume.rapin@unige.ch)
(Dated: November 2, 2021)

A. PFM measurements of domain growth at electrode edges

To follow the growth of the down-polarised domains into the up-polarised as-grown regions of the sample, vertical piezoresponse force microscopy (PFM) imaging was carried out in a Bruker Dimension V AFM system at ambient conditions, using Bruker MESP tips, with a 20 kHz drive frequency, 3000 mV drive amplitdue, and 3 μm/s tip scanning velocity). After the application of a 10 V switching pulse for the chosen duration, concurrent PFM phase and amplitude 5×5 μm^2 images were taken along the electrode edge with a 1024×1024 pixel resolution, as can be seen in Figs. S1– S4 for domains switched at 23° C and 100° C, respectively. Given the intrinsically almost perfectly binary nature of phase imaging (180° phase difference with relatively low noise) with a steep change between the two phase states corresponding to up- vs. down-polarised domains, convoluted essentially only by the tip size, vertical PFM phase provides the most reliable and least noisy way to precisely determine the domain wall position. The amplitude channel can be used, tracking its minimum as the position of the domain wall in each scan line, and gives comparable domain wall geometry, but with far more noise. This is because the amplitude channel is more prone to variability via electrostatic and electrochemical effects, and as a result of contact resonance variations giving rise to crosstalk with the sample topography.

B. Image processing

Each of the 1024×1024 px vertical PFM phase images, with phase values normalised on a 0–360° range, were offset to obtain comparable minimum values (centered around 180°, crimson colour in Figs. S1,S3) for the as-grown up-polarised domains, and maximum values (centered around 360°, yellow colour in Figs. S1,S3) for the down-polarised domains growing outwards from the electrode edges. The images were then binarised using in-house developed algorithms within the Hystorian materials science data analysis Python package [1], allowing the positions of the electrode edges and domain walls to be identified, and their x, y coordinates extracted. Finally, the relative front displacement $u(z)$ was obtained as the difference in the x coordinates of the electrode edge and domain wall for each y coordinate value.

C. Modelling electric field intensity at electrode edges

When voltage pulses are applied across a ferroelectric film sandwiched between macroscopic electrodes in a planar capacitor geometry, as schematically illustrated in Fig. S5(a–c), previous studies have shown that polarisation switching proceeds by the nucleation, growth, and coalescence of multiple domains [2, 3] in the intense, homogeneous and purely out-of-plane electric field within the capacitor. Once the ferroelectric volume within the capacitor is fully switched into the polarisation state orientated parallel to the applied electric field, much slower outward domain growth is possible, driven by the fringing fields extending beyond the edges of the electrodes.

Using Comsol finite element 2D (slab) simulations of a 270 nm thick, 10 μm long PZT film with its lower boundary fixed at ground, and a 55 nm thick, 5 μm wide perfectly conducting top electrode to which 10 V potential could be applied, we numerically simulated the fringing electric field to extract its out-of-plane component, shown in Fig. S6(a). As can be seen in Fig. S6(b), the intensity of the fringing fields decreases very rapidly as a function of distance from the electrode edge. We therefore expect progressively slower domain wall motion and less significant effects of surface and bulk charge dynamics as the domain walls are driven further from the electrodes.

D. Extracting the creep exponent μ

The domain wall velocity during creep depends on both the temperature T and the vertical component of the electric field E_z which drives the motion. We therefore carried out a self-consistent two-dimensional surface fitting of the creep equation (Eq. 1 of the main text) to the cloud of points combining data obtained from switching at both 23° C and 100° C, as shown in Fig. S6(a). Seed values for the two-dimensional fitting parameters were obtained from fits carried out separately on the datasets obtained at the two different temperatures, shown for comparison in Fig. S6(b). Based on these preliminary values, the two-dimensional fits were processed using the Python *Scipy* library and the *curve_fit* function.

---

* These authors contributed equally to this work
† These authors contributed equally to this work; Now at DACM, State of Geneva, Switzerland
‡ Now at Federal Institute of Metrology METAS, Switzerland

E. Multiscaling analysis of the probability distribution function of relative displacements

The statistical distribution of the fluctuation of the domain wall position can be quantified by defining the probability distribution function (PDF) of the relative displacements $\Delta u(r,z)$ at a given length scale r

$$P[\Delta u(r,z)] = \frac{1}{N}\int dz \cdot \Delta u(r,z) \tag{S1}$$

where the factor N ensures normalisation. The central moments of this PDF, reflecting its characteristic scaling properties [4], are the real-space displacement autocorrelation functions

$$\sigma_n(r) = \overline{\langle|\Delta u(r)|^n\rangle} \sim r^{n\zeta_n}, \tag{S2}$$

where ζ_n are the associated scaling exponents for the nth moment.

For monoaffine systems, such as 1-dimensional equilibrated interfaces at zero temperature in weak collective pinning, the PDF is well approximated by a Gaussian function [5–7], and the second moment or roughness $B(r) \equiv \sigma_2(r) \sim r^{2\zeta}$ is sufficient to fully characterise the scaling, with a single-valued exponent $\zeta_n = \zeta\ \forall n$. For multiaffine systems, such as out-of-equilibrium, correlated disorder, or strong pinning scenarios [8–10] the full set of higher order scaling exponents $\zeta_n \neq (n/2)\zeta_2$ are necessary to characterise the interface roughening.

To investigate the nature of the domain walls and the symmetry of their relative displacements, we therefore carried out a multiscaling analysis [11, 12] to evaluate their PDF and its central moments. As shown in Figs. S8 (a–d) and S9(a–d), the PDFs obtained for different r values and switching pulse durations for domain walls written at 23° C and 100° C, respectively, are generally quite symmetric. The corresponding renormalised central moments, shown in Figs. S8 (e–h) and S9(e–h)

$$C_n(r,z) = [\sigma_n(r,z)]^{1/n} \tag{S3}$$

show some fanning at the highest and lowest r values, but collapse to within 15 % in the intermediate range.

[1] L. Musy, R. Bulanadi, I. Gaponenko, and P. Paruch, Ultramicroscopy , 113345 (2021).
[2] S. Hong, E. L. Colla, E. Kim, D. V. Taylor, A. K. Tagantsev, P. Muralt, K. No, and N. Setter, J. Appl. Phys. **86**, 607 (1999), https://doi.org/10.1063/1.370774.
[3] A. Gruverman, D. Wu, and J. F. Scott, Phys. Rev. Lett. **100**, 097601 (2008).
[4] E. Agoritsas, V. Lecomte, and T. Giamarchi, Phys. B **407**, 1725 (2012).
[5] T. Halpin-Healy, Phys. Rev. A **44**, R3415 (1991).
[6] M. Mézard and G. Parisi, J. de Phys. I **1**, 809 (1991).
[7] A. Rosso, R. Santachiara, and W. Krauth, J. Stat. Mech. , L08001 (2005).
[8] T. Nattermann, Y. Shapir, and I. Vilfan, Phys. Rev. B **42**, 8577 (1990).
[9] A.-L. Barabasi, R. Bourbonnais, M. Jensen, J. Kertesz, T. Vicsek, and Y.-C. Zhang, Phys. Rev. A **45**, R6951 (1992).
[10] A. B. Kolton, A. Rosso, and T. Giamarchi, Phys. Rev. Lett. **95**, 180604 (2005).
[11] S. Santucci, K. J. Måløy, A. Delaplace, J. Mathiesen, A. Hansen, J. Ø. H. Bakke, J. Schmittbuhl, L. Vanel, and P. Ray, Physical Review E **75** (2007).
[12] J. Guyonnet, E. Agoritsas, S. Bustingorry, T. Giamarchi, and P. Paruch, Physical Review Letters **109** (2012), 10.1103/physrevlett.109.147601.

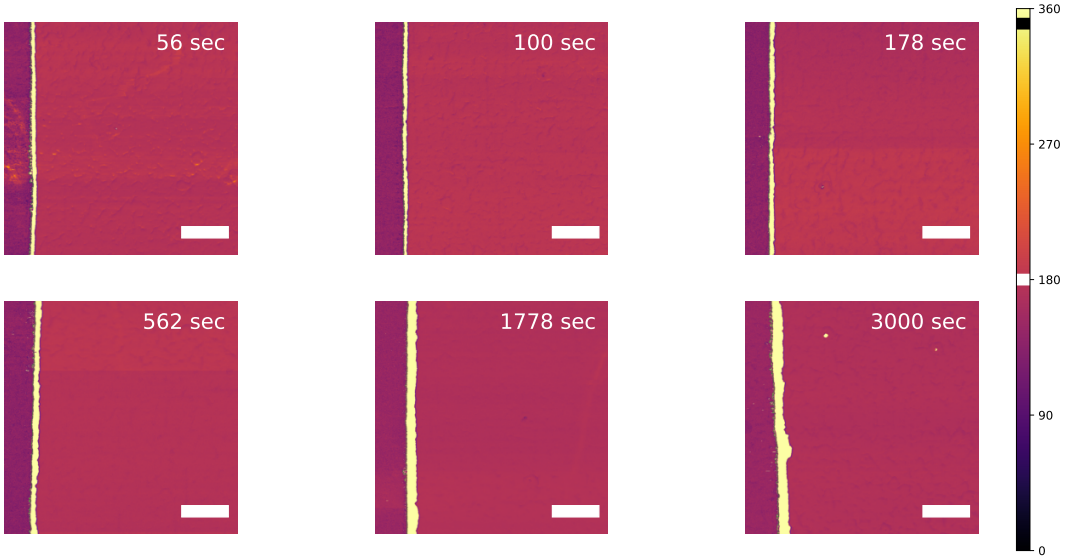

FIG. S1: *PFM phase images of domain growth at electrode edges at 23°C.* Domains written with 10 V pulses applied to the top electrode for the indicated switching pulse duration. The white bar represents 1 μm, and all images are shown at the same PFM phase scale, with the white and black regions on the scale representing the approximate value of the down and up polarised domains, respectively.

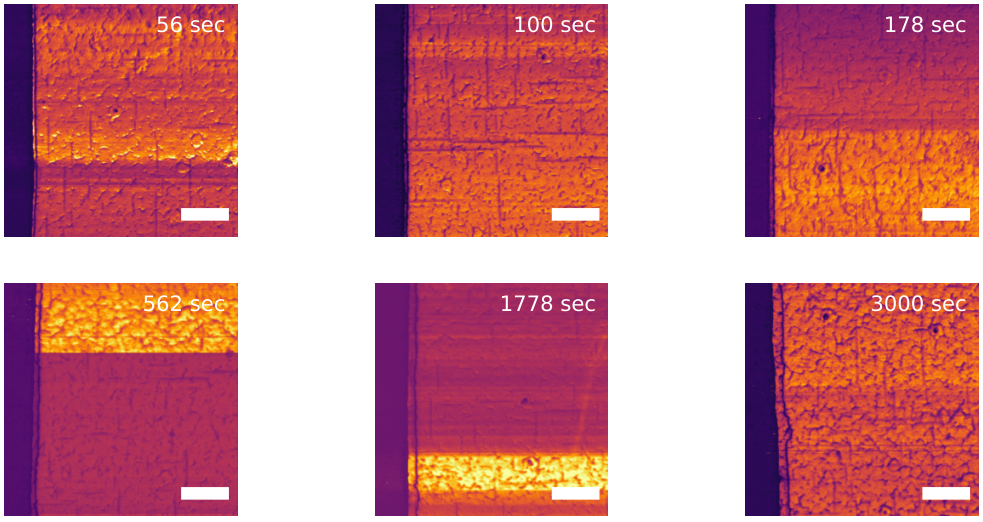

FIG. S2: *PFM amplitude images of domain growth at electrode edges at 23° C.* Acquired concurrently with the measurements shown in Fig. S1, the amplitude images recapitulate the same information, with the 180° domain walls visible as a narrow dark line to the right of the electrode, itself corresponding to a region of minimum amplitude at the left of each image, since it blocks our PFM signal. The white bar represents 1 μm.

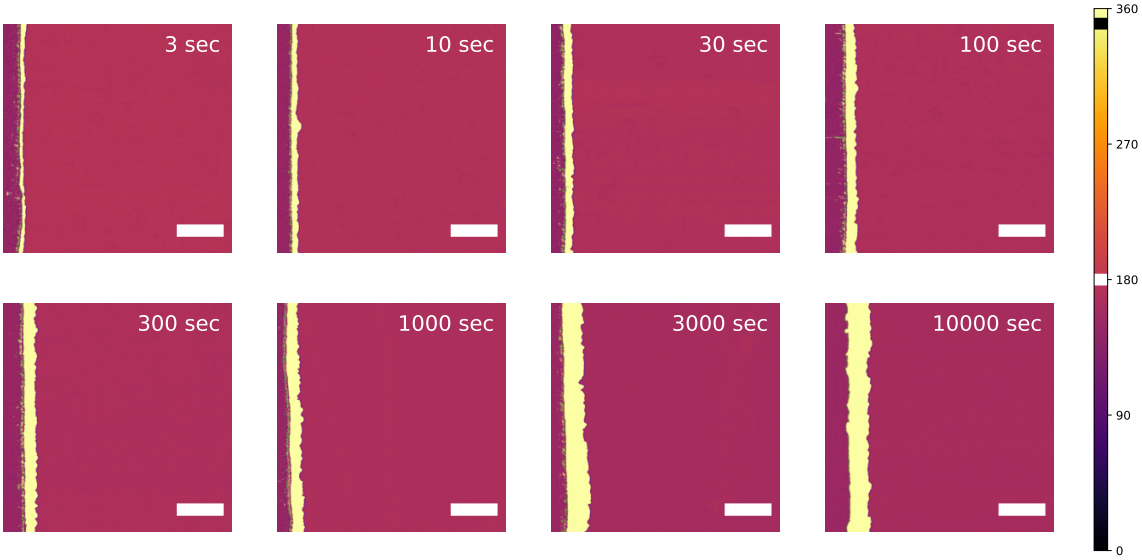

FIG. S3: *PFM phase images of domain growth at electrode edges at 100° C.* Domains written with 10 V pulses applied to the top electrode for the indicated switching pulse duration. The white bar represents 1 μm, and all images are shown at the same PFM phase scale. with the white and black regions on the scale representing the approximate value of the down and up polarised domains, respectively.

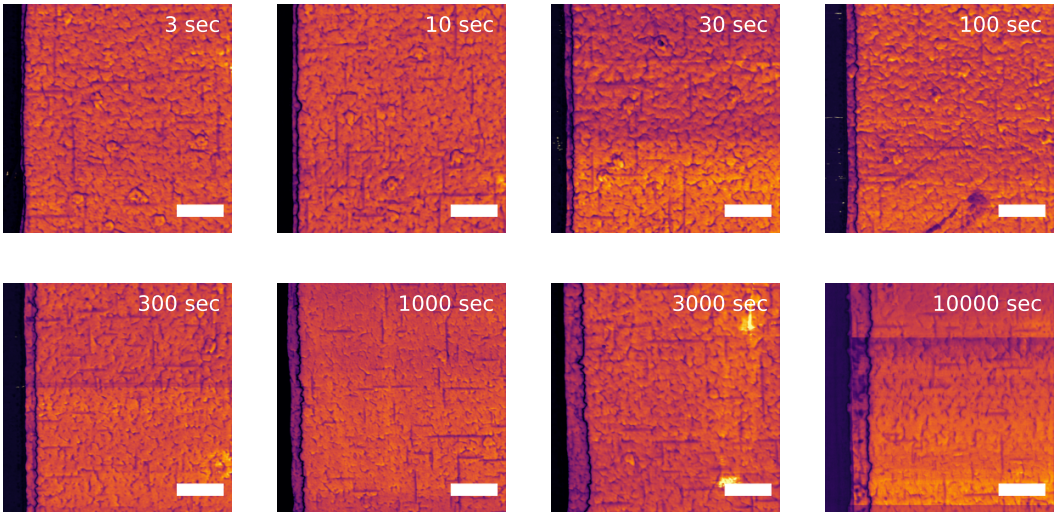

FIG. S4: *PFM amplitude images of domain growth at electrode edges at 100° C.* Acquired concurrently with the measurements shown in Fig. S3, the amplitude images recapitulate the same information, with the 180° domain walls visible as a narrow dark line to the right of the electrode, itself corresponding to a region of minimum amplitude at the left of each image, since it blocks our PFM signal. The white bar represents 1 μm.

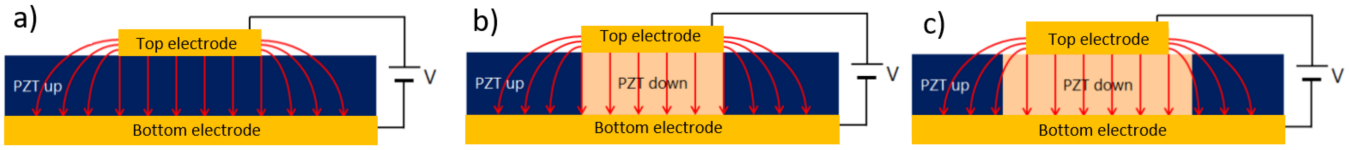

FIG. S5: *Schematic representation of polarisation reversal in a planar capacitor geometry* (a) The initially up-polarised PZT thin film, with a $SrRuO_3$ epitaxial bottom electrode and Au/Ti patterned top electrodes, between which 10 V pulses are applied, giving rise to uniform, out-of-plane, high intensity electric field under the top electrode, and fringing fields extending from its edges (field lines represented in red). As a result, initial domain nucleation and growth occurs directly under the top electrode (b), followed by propagation of domain walls away from the electrode edges (c).

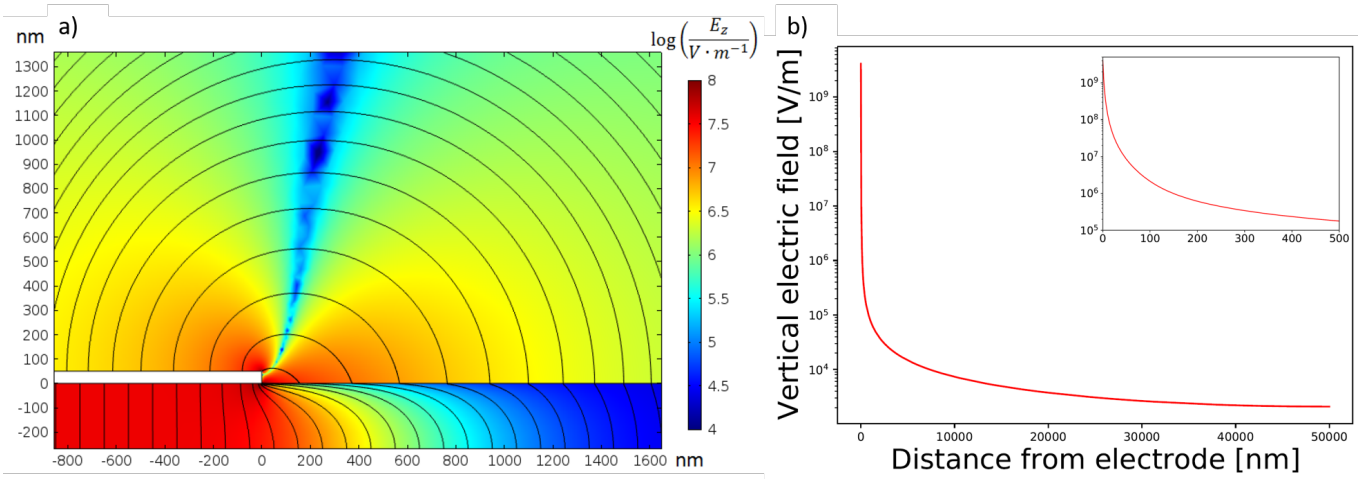

FIG. S6: *Electric field driving domain wall dynamics at electrode edges* (a) Finite element simulation of the out-of-plane component of the electric field E_z in the planar capacitor geometry of the measurements, and (b) the corresponding values of E_z extracted at the ferroelectric surface, as a function of the distance from the electrode edge. The inset shows the E_z values at length scales corresponding to the width of the domains imaged in our experiments.

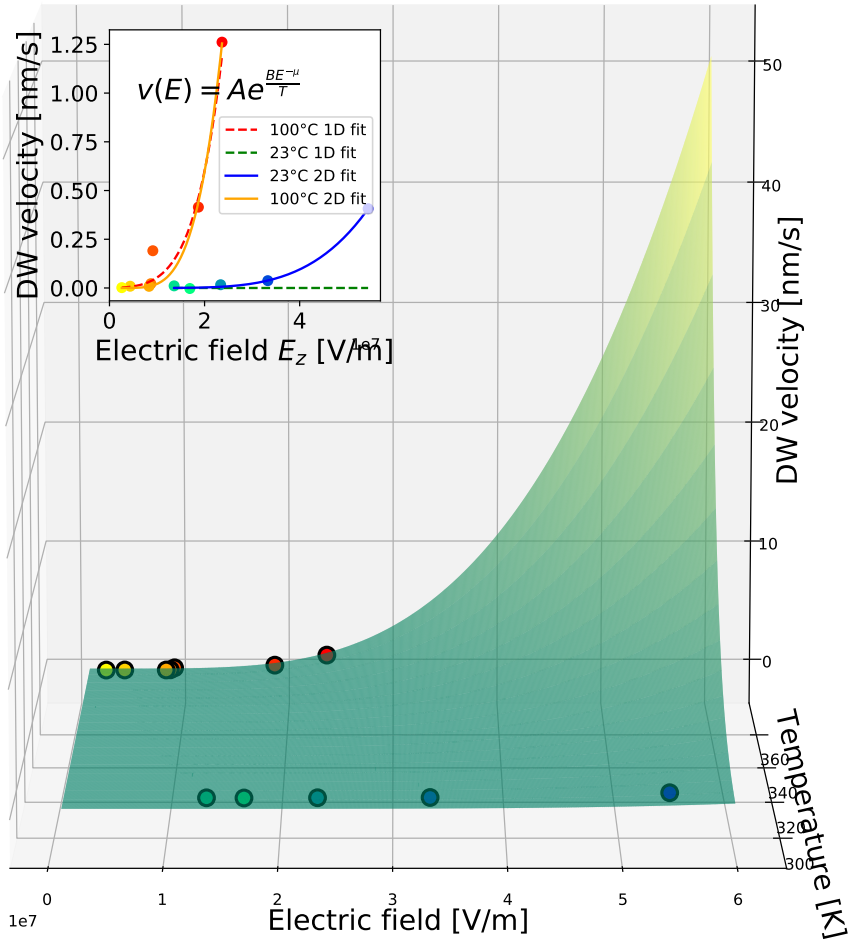

FIG. S7: *Fitting domain wall motion as a creep process* $v(E) = e^{\frac{-U_c}{k_B T}(\frac{E_c}{E})^{\mu}}$ Domain wall velocity as a function of the out-of-plane electric field and temperature, self-consistently fitting the data obtained at both 23° C and 100° C as a two-dimensional surface. The inset shows domain wall velocity as a function of the out-of-plane component of the electric field at the edge of the electrode, where solid lines are extracted from the two-dimensional fit, and the dashed lines from fits done separately on the data obtained at the two different temperatures. 23° C data are shown on the blue–green colour scale, and 100° C data on the red–yellow colour scale.

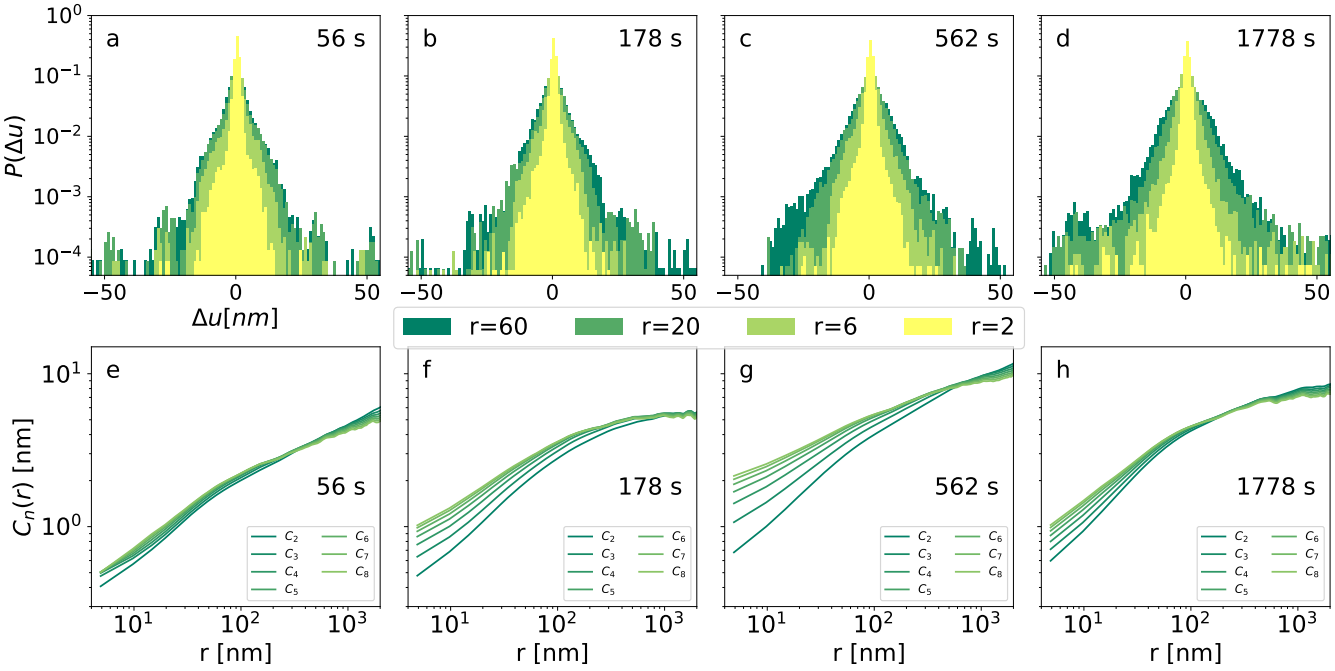

FIG. S8: *Multiscaling analysis for domain walls written at 23° C* (a–d) Probability distribution function of relative displacements $\Delta u(r,z)$ for $r \in 6, 40, 60, 400$ nm and (e–h) power law scaling of its averaged renormalised central moments C_2–C_8, for domain walls written with switching pulse duration of 56, 178, 562, and 1778 s.

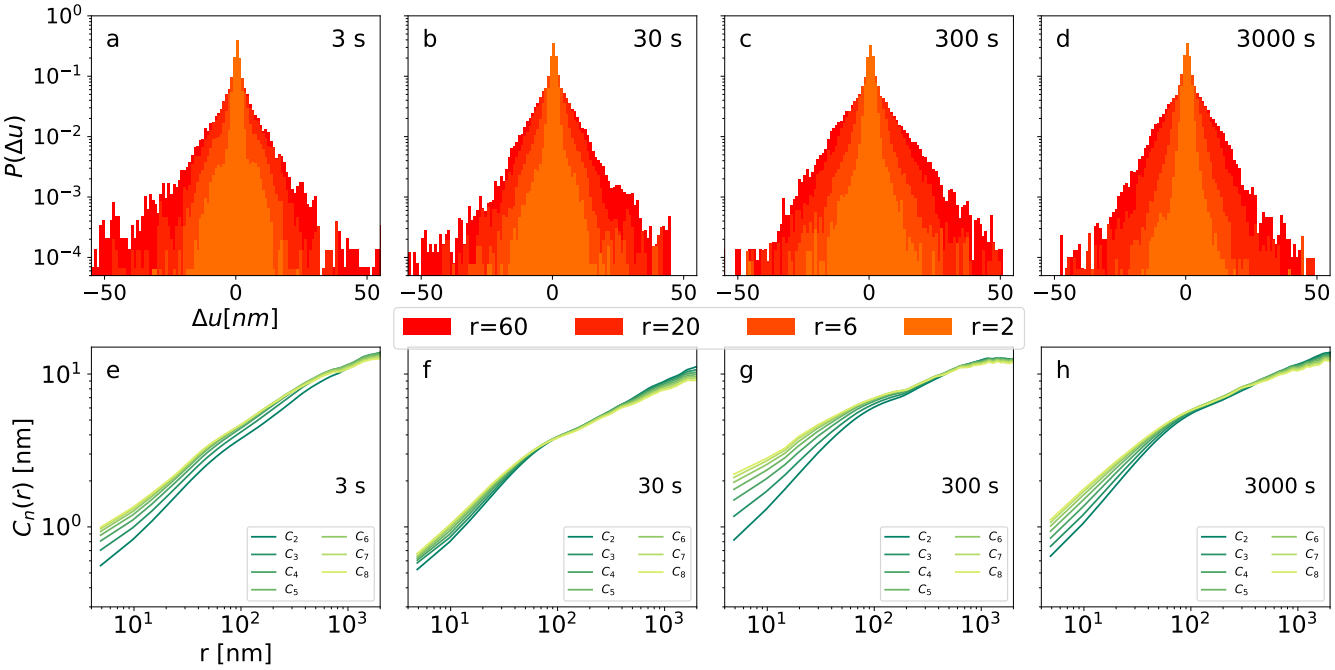

FIG. S9: *Multiscaling analysis for domain walls written at 100° C* (a–d) Probability distribution function of relative displacements $\Delta u(r,z)$ for $r \in 6, 40, 60, 400$ nm and (e–h) power law scaling of its averaged renormalised central moments C_2–C_8, for domain walls written with switching pulse duration of 3, 30, 300, and 3000 s.